Desalination and Water Treatment
www.deswater.com

doi: 10.5004/dwt.2019.24067

154 (2019) 376–384
June

Adsorption of crystal violet onto epichlorohydrin modified corncob

Yinghua Song*, Rong Peng, Shengming Chen, Yaqian Xiong

Department of Chemical Engineering, Chongqing Key Lab of Catalysis and Functional Organic Molecules, Chongqing Technology and Business University, Chongqing 400067, China, Tel. +86-023-62769785; Fax: +86-023-62769785; emails: yhswjyhs@126.com (Y. Song), pengrong@ctbu.edu.cn (R. Peng), chensm@ctbu.edu.cn (S. Chen), xiongyq@ctbu.edu.cn (Y. Xiong)

Received 20 October 2018; Accepted 28 February 2019

ABSTRACT

A novel low-cost biosorbent, corncob modified with epichlorohydrin, was used to remove crystal violet (CV) from its aqueous solution. The influences of process parameters, such as initial pH, temperature, contact time and initial CV concentration on its adsorption capacity were investigated in a batch system. The equilibrium data were evaluated using the Langmuir and the Freundlich isotherms, and the former could provide a better fit with the q_{max} of 71.43 mg g^{-1} at 318 K. A new method derived from the Langmuir equilibrium constant K_L was first put forward to estimate the thermodynamics. The obtained negative values of ΔG demonstrated a spontaneous process of CV onto corncob. The adsorption kinetics could be well described by the pseudo-second-order model. It was concluded that the intra-particle diffusion was one of the rate-controlling steps in this process. The corncob modified with epichlorohydrin was proved to be a promising adsorbent to treat dye wastewater.

Keywords: Adsorption; Corncob; Crystal violet; Thermodynamics; Mechanism; Epichlorohydrin

1. Introduction

Dyes and pigments are widely utilized in a variety of industries to color their products, including printing, textiles, leather, paper, plastics, food, etc. Among these dyes, many are difficult to be biodegraded because of their complicated structures and properties. Besides, some dyes, especially azo dyes, are either toxic, teratogenic, or even carcinogenic [1]. The direct discharge of such dye wastewater will cause serious safety hazards and environmental problems. CV, a cationic dye, is often used for instance biological marker, veterinary drugs and dermatological agents. Signs have shown that CV may cause queasiness, hemolysis, hypertension and respiration suffering and many other health problems or environmental issues [2].

At present, many technologies have been developed to remove dyes from wastewater, including advanced oxidation, aerobic and anaerobic digestion, adsorption, membrane filtration and flocculation [3]. Among these methods, adsorption shows good performance for the treatment of dye wastewater. Activated carbon has become the most widely used adsorbent to remove dyes because it shows good adsorption property and chemical stability. Since the operation cost is still very expensive, people are trying to find more economical and efficient adsorbents to accomplish it. And now an alternative has been successfully explored from different agricultural and forestry wastes such as peanut husk [4,5], banana peel [6], saw dust [7], coconut coir dust [8], internal almond shell [9], walnut shell [10], etc.

Corncob, an abundant agricultural residue, has been successfully used to remove contaminants from wastewater due to its good adsorption property, excellent mechanical strength and good chemical stability. Efficient removal of copper ions [11] has been achieved by introducing native corncob as a low-cost adsorbent directly. However,

* Corresponding author.

1944-3994/1944-3986 © 2019 Desalination Publications. All rights reserved.

because of two major limitations, raw corncob may not be suitable for use as a good natural adsorbent. First, the soluble component in the corncob will dissolve in water, and make the water appear light yellow; second, long-term contact with water will cause the corncob to be dispersed in the bulk solution. Researchers found that the adsorption performance of the corncob toward different dyes could be efficiently improved by chemical modification [12–14]. Epichlorohydrin was widely used as a modification reagent to improve the adsorption capacity of various adsorbents, such as starch [15], corn stalk [16], alginate guar gum matrix [17] and so on. Peanut husk was also modified with epichlorohydrin by our team [5], and the prepared adsorbent was used to remove carmine from aqueous solution. The adsorption capacity was found to be improved significantly. Epichlorohydrin was, therefore, chosen to modify corncob chemically in this work and the impacts of pH, the initial CV concentration, temperature and contact time on the adsorption of CV on the prepared adsorbent were investigated. The mechanisms were deduced with equilibrium, kinetics and thermodynamics. A new method derived from the Langmuir equilibrium constant K_L was first proposed to estimate the thermodynamics. The aim of this work is to develop an economic and promising biosorbent from corncob for removal of dyes in wastewater.

2. Materials and methods

2.1. Preparation of epichlorohydrin modified corncob

The corncob used in this work was purchased from a local farmers' market. The raw material was first soaked in water for 24 h and then rinsed thoroughly with deionized water to remove impurities dissoluble in water. After that, it was placed in an air circulating oven and dried for 24 h at 60°C. In order to obtain the adsorbent with uniform particle size, it was grounded and sieved below 60 mesh size.

40 mL of epichlorohydrin (AR) and 45 mL of NaOH solution (1.25 mol L^{-1}) were mixed with 2.0 g of the raw corncob. Then the mixture was placed in a water bath to react for 0.5 h at the temperature of 45°C ± 1°C. The obtained epichlorohydrin modified corncob (EMC) was filtered and rinsed thoroughly with distilled water until the effluent was neutral. And it was finally dried in an oven for 24 h at 60°C and kept in a dryer.

The modification process can be expressed as Fig. 1 [18].

2.2. Chemicals

1.0 g of CV was dissolved into 1 L of double-distilled water to prepare the stock solution, which was then diluted to the desired concentration ranging from 50 to 200 mg L^{-1} to prepare sample solutions. The initial pH of sample solutions was adjusted to a preset value (1.00–12.00) ± 0.10 through 1.0 mol L^{-1} of the sodium hydroxide or hydrochloric acid solution before the adsorbent was added.

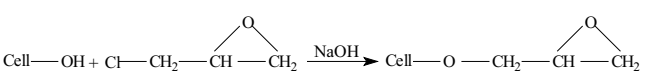

Fig. 1. General reaction scheme.

2.3. Batch adsorption procedure

0.2 g of EMC was added to 100 mL of CV solutions at the desired concentration in conical flasks, which were agitated on a shaker at 100 rpm. Test samples were taken from the mixture to determine the residual concentration of CV solution at 574 nm spectrophotometrically. All experiments were completed three times to ensure the accuracy of the data and average values were used for subsequent calculation.

The adsorption capacity q (mg g^{-1}) was calculated using Eq. (1).

$$q = \frac{v\left(C_0 - C_t\right)}{m} \tag{1}$$

where C_0 (mg L^{-1}) is the initial concentration, C_t (mg L^{-1}) is the concentration at time t, v (L) is the volume of CV solution and m is the weight of the EMC used (g).

2.4. Adsorption kinetic studies

Several successive steps are usually involved in adsorption process and kinetic studies may help us to find the rate controlled step. For this purpose, experimental data were compared with those predicted by the pseudo-first-order [19] and pseudo-second-order models [20]. Besides, the intraparticle diffusion kinetics proposed by Weber and Morris [21] was also used to determine the rate-controlling step. The three kinetic models are given by Eqs. (2)–(4).

$$q_t = q_e\left(1 - e^{-k_1 t}\right) \tag{2}$$

$$q_t = \frac{k_2 q_e^2 t}{1 + k_2 q_e t} \tag{3}$$

$$q_t = K_p t^{1/2} + C \tag{4}$$

where q_t (mg g^{-1}) is the adsorption capacity at time t (min^{-1}), q_e (mg g^{-1}) is the calculated capacity. k_1 (min^{-1}) is the rate constant for the first order, k_2 (g mg^{-1} min^{-1}) is the rate constant for the second order, K_p (mg $min^{-1/2}$ g^{-1}) is the rate constant for the intraparticle diffusion models and C (mg g^{-1}) is a parameter related to the boundary layer.

For kinetic studies, 0.2 g of EMC was added to a series of flasks containing 100 mL of CV solutions with the same initial CV concentration, an individual flask was taken out to measure the residual concentration at each pre-determined time interval.

2.5. Adsorption equilibrium studies

Information about adsorption capacity and interaction force between the adsorbent and the adsorbate can be found from adsorption isotherms. The most widely used isotherms, namely, the Langmuir and Freundlich isotherms were used to describe the present system in this work [22,23]. Non-linear forms of adsorption isotherms were presented as follows:

$$q_e = \frac{q_{\max} K_L C_e}{1 + K_L C_e} \tag{5}$$

$$q_e = k_f C_e^{1/n} \tag{6}$$

where C_e (mg L^{-1}) is the equilibrium CV concentration, q_e (mg g^{-1}) is the capacity at equilibrium, q_{max} (mg g^{-1}) is the maximum Langmuir adsorption capacity, K_L (L mg^{-1}) is the Langmuir equilibrium constant, k_f (L mg^{-1}) is the Freundlich equilibrium constant and n (dimensionless) is a constant related to the heterogeneity of the adsorbent.

For isotherm studies, 0.1 g of EMC was added to several flasks containing 50 mL of CV solution at the desired concentration. The adsorption was conducted at temperatures of 298, 308 and 318 K for 24 h, respectively.

The kinetic and isotherm data were non-linearly fitted using the software of Microcal OriginPro 8.5.1.

2.6. Thermodynamic studies

Thermodynamic analysis of the equilibrium data may shed light on the mechanism of the adsorption process. The thermodynamic parameters, such as free energy change (ΔG), enthalpy (ΔH) and entropy change (ΔS), can be computed under the help of Eq. (7) [24].

$$\Delta G = \left(\Delta H - T\Delta S\right) = -RT\ln K_e \tag{7}$$

where K_e is the equilibrium constant (dimensionless), R is the universal gas constant (8.314 J mol^{-1} K^{-1}) and T is the absolute temperature (K).

Obviously, the key factor to determine the thermodynamic parameters with Eq. (7) is the correct calculation of K_e, which have been estimated using different methods. From these various procedures, the Langmuir constant K_L and partition coefficient K_p were chosen as the reference to calculate K_e.

Many scientists used the K_L and k_f constants of the Langmuir and the Freundlich isotherms instead of the K_e directly [25–27], but we can see from Eq. (7), K_e should be a dimensionless parameter. $K_L \approx K_e$ was considered to be acceptable when the solute activity can be negligible only if the solution of the ionic solute was very dilute or the solute was a non-ionic one [28]. It was suggested that K_L could be converted to a dimensionless K_e with Eq. (8) when K_L is expressed as L mg^{-1} [4,5,28,29] in aqueous solution. This calculation method has been recommended to be more accurate than the direct use of K_L [29]. And therefore, we also calculate K_e with Eq. (8) as a reference.

$$K_{e1} = 10^6 K_L \tag{8}$$

Recently, partition or distribution coefficient K_p, q_e/C_e or C_a/C_e (where C_a is the concentration of solute adsorbed onto the adsorbent), was often utilized directly as K_e [30–32], but the dimensionless one could be only obtained with Eq. (9) by plotting $\ln(C_a/C_e)$ vs. C_a and extrapolating to $C_a = 0$. If the plot is a straight line with a high correlative coefficient (R^2), K_p can be used as the correct value of K_e [29,33].

$$K_{e2} = K_p = \lim_{C_a \to 0} \frac{C_a}{C_e} \tag{9}$$

As can be seen from the Langmuir isotherm, the unit of K_L should be L mg^{-1} when the C_e is in mg L^{-1}. It can be certainly changed into a dimensionless parameter by multiplying with a variable in mg L^{-1}, for example, 10^6 mg L^{-1}, the pure water concentration when the adsorbate was dissolved in water. But from the relationship q_e/C_e, it should be more reasonable that the unit of K_L be mg (adsorbate) mg^{-1} (adsorbent) over mg (adsorbate) L^{-1} (solution), that is, L (solution) mg^{-1} (adsorbent). The Langmuir equilibrium constant K_L can be converted into a dimensionless one by multiplying with mg (adsorbent) L^{-1} (solution) conducted in the system under investigation. Since 0.1 g of EMC was added into 50 mL of solution in the present equilibrium study, we got the K_{e3} by multiplying the K_L with 2,000 mg L^{-1} (i.e., 0.1 g/50 mL) as Eq. (10).

$$K_{e3} = 2{,}000K_L \tag{10}$$

ΔG was calculated using the following equation since the present adsorption process could be well described by the Freundlich isotherm [34].

$$\Delta G = -nRT \tag{11}$$

where n is the Freundlich constant.

3. Results and discussion

3.1. Characterization of EMC

3.1.1. FT-IR

The functional groups of the raw corncob and EMC are shown in the FT-IR spectra (Fig. 2). The two spectra presented similar characteristics and adsorption peaks. The strong and broad peak around 3,400 cm^{-1} could be assigned to the O–H groups, carboxylic groups or amide N–H stretching, corresponding to the vibration of functional groups in cellulose or hemi-cellulose [35]. The adsorption peak at 2,925 cm^{-1} was reported to be the symmetric or asymmetric stretching vibration of C–H bonds in CH_2 and CH_3 groups. The peak located at approximately 1,700 cm^{-1} was attributed to the stretching vibration of C=O in carboxylic acids. The peak that mostly characterizes epoxide groups observed around 1,100 cm^{-1} has high intensity for EMC when compared with the raw corncob, which indicated that the modification reaction of epichlorohydrin was successfully accomplished.

3.1.2. XRD

The XRD of EMC (Fig. 3) showed a similar result to that of raw corncob with the same diffraction peak. The most remarkable highlighted that characteristic sharp intensity diffraction peaks at 2θ values of 17°, 22.5° and 35° which reflect the crystalline nature of cellulose [15]. The modification with epichlorohydrin did not change the structure of cellulose.

3.2. Effect of initial pH of solution

pH of the solution affects the interaction force between the adsorbent and the adsorbate. The effect of pH on the adsorption of CV onto EMC was studied in the range of 2–12. The results obtained are presented in Fig. 4.

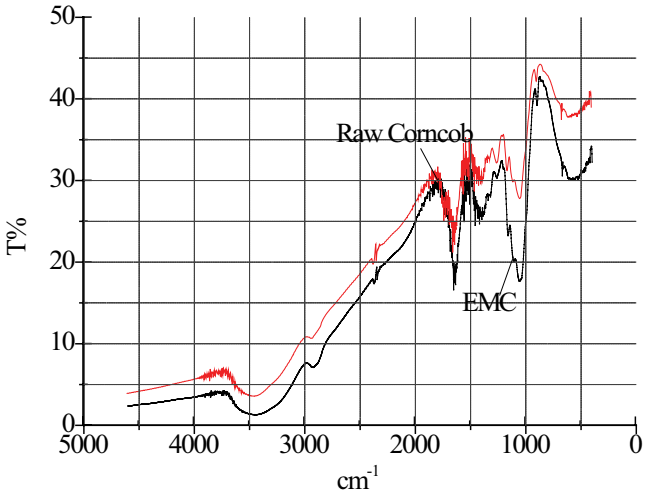

Fig. 2. FT-IR of raw corncob and EMC.

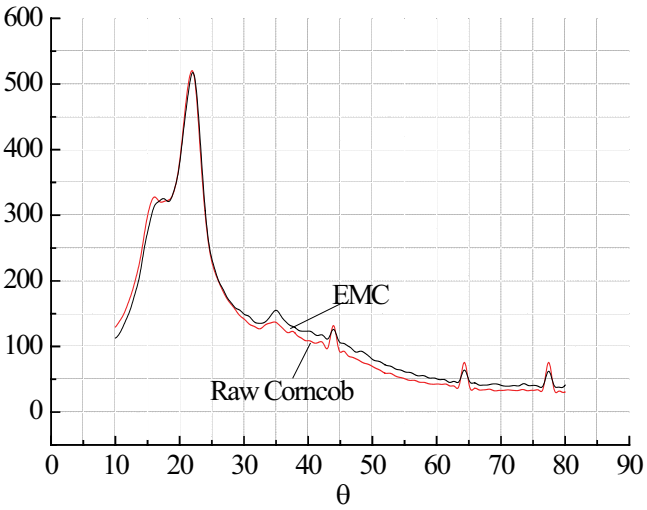

Fig. 3. X-ray diffractograms of raw corncob and EMC.

As shown in Fig. 4, the adsorption capacity of CV increased sharply as the pH increased from 2.0 up to 4.0, then it increased gradually until the maximum adsorption capacity of 49.08 mg g^{-1} was obtained at pH 8.0. As pH increased further, CV adsorption decreased again. As a cationic dye, the adsorption of CV may be hindered by enhanced protonation of $–NH_2$ on the surface of the EMC at low pH. With increasing pH, protonation reduced and electrostatic attractive force became dominant, which was preferential for the adsorption of the positive CV ions to negative active sites. The successive decreasing trend under basic condition (pH > 8) was due to the formation of hydroxyl species. Similar results for the pH effect on the CV adsorption have been reported in the literature [36,37].

The effect of pH on the CV adsorption has also been examined on the basis of the point of zero charge (pH_{pzc}) of EMC. The pH_{pzc} is the point where the curve ($pH_{initial}$–pH_{final}) against $pH_{initial}$ intersect the abscissa and then the $pH_{initial}$ = pH_{final} (Fig. 5). In order to determine the pH_{pzc}, 0.2 g EMC was transferred into a 100 mL flask containing 50 mL of

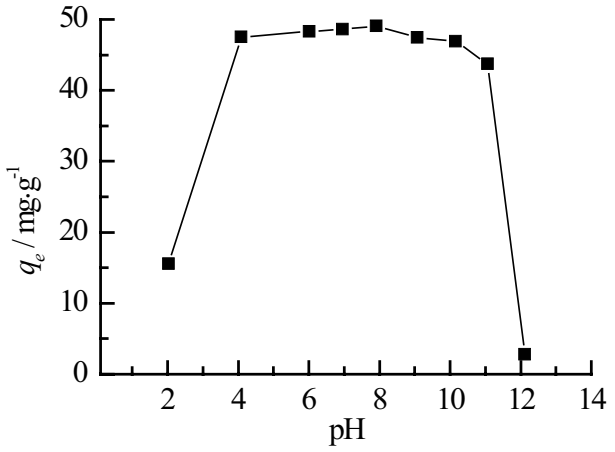

Fig. 4. Effect of pH on the adsorption of CV (T = 298 K, C_0 = 95.6 mg L^{-1}, contact time = 24 h, rpm = 100).

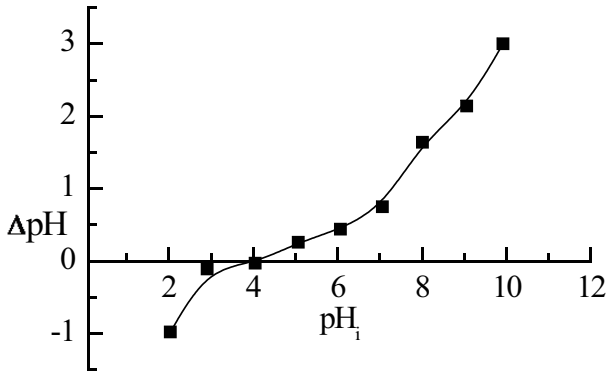

Fig. 5. pH of the point of zero charge of EMC.

0.01 mol L^{-1} NaCl. The $pH_{initial}$ was adjusted to 2–10 by the addition of 0.1 mol L^{-1} HCl or 0.1 mol L^{-1} NaOH. The flask was sealed and placed into a shaker for 48 h under atmospheric conditions and the pH_{final} of the solution was then measured. From Fig. 5, the pH_{pzc} of EMC was established to be 4.06. This implies that at pH < pH_{pzc}, the surface of EMC is protonated by the absorption of H^+ ions resulting in an electrostatic repulsion with the cationic CV dye [38]. Further, at pH > pH_{pzc}, EMC surface bears the negative charges which causes an electrostatic attraction between the cationic dye. This clearly indicates that for the adsorption of CV, the pH of the adsorption system should be greater than 4.06 when EMC was used as the adsorbent.

3.3. Adsorption kinetic studies

3.3.1. Effect of contact time

CV removal by EMC was conducted with the initial CV concentrations varied from 78.6 to 212.5 mg L^{-1} at temperature 298 K as shown in Fig. 6.

Adsorption of CV proceeded very fast in the first 2.5 h and then tapered off until reaching equilibrium finally at about 24 h. The initial high rate was due to lots of vacant sites existed on the surface of EMC at first. Then with increasing time, these vacant sites were gradually occupied,

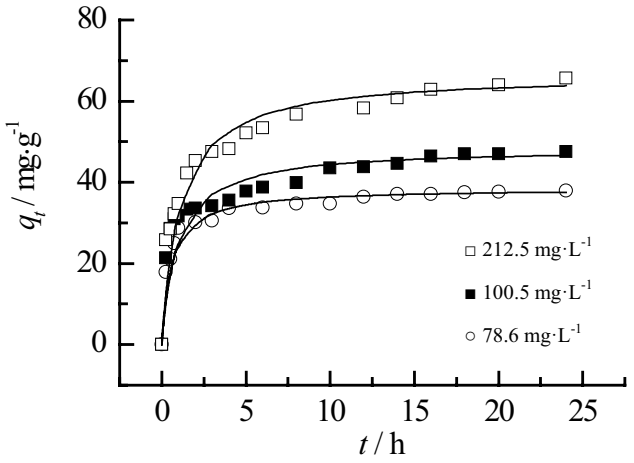

Fig. 6. Effect of contact time on the adsorption of CV (T = 298 K, pH = 8.0 ± 0.1, rpm = 100). The lines represented the best non-linear regression fits with pseudo-second-order kinetics.

the repulsive forces between CV molecules and solution increased, the adsorption process became slower [39]. The equilibrium capacity of the EMC increased from 38.64 to 66.94 mg g^{-1} when the initial CV concentration increased up to 212.5 mg L^{-1} because of an important driving force provided with higher concentration [40].

3.3.2. Kinetic studies

The adsorption of CV dye vs. time data was tested against various available kinetic models. The kinetic parameters, k_1, k_2 and q_e, gotten by non-linear regression analysis of Eqs. (2) and (3) were compared in Table 1, together with the correlative coefficients R^2. It was observed that the correlative coefficients of the pseudo-first-order model were rather low. Furthermore, big gaps between the calculated and the experimental equilibrium capacities were found. All these suggested that CV adsorption did not conform to the pseudo-first-order model.

The non-linear fit of the pseudo-second-order model is also presented in Fig. 6. This model seemed to give a much better fit for CV adsorption onto EMC when compared with the pseudo-first-order model, this behavior is supported by the high correlative coefficient $R^2 > 0.995$ and the perfect agreement between $q_{e,cal}$ and q_{exp}. Given that, a chemical interaction between CV and EMC based on electron exchange or charge sharing may happen besides physical adsorption in this process. Similar results have been reported for malachite green adsorption onto modified sphagnum peat moss [41]. The kinetic rate constant k_2 decreased with increasing initial CV concentrations (Table 1) because of the competition for the limited surface of adsorption sites was intensified with increasing CV concentrations.

As shown in Fig. 7 and Table 1, the adsorption kinetics of CV on EMC could be described by three-linear characteristics. The q_t in the first portion increased rapidly with time due to the fast film mass transfer of CV from the bulk solution to the surface of EMC. During this stage, the active sites on the EMC surface were freely available for CV molecules, and the boundary thicknesses (C_1) were also less. The second portion demonstrated an intraparticle diffusion from the outer surface to the inside of EMC [42,43]. And the last section represented the gradual adsorption to equilibrium.

Table 1
Statistical results of the application of the kinetic models

Model			Initial CV concentration/mg L^{-1}		
			78.6	100.5	212.5
First order kinetic	k_1	Rate constant, h^{-1}	1.87	1.93	1.04
	$q_{e,cal}$	Equilibrium capacity, mg g^{-1}	35.16	41.22	57.20
	R^2	Correlative coefficient	0.9334	0.8236	0.8782
Second order kinetic	k_2 (10^{-2})	Rate constant, g mg^{-1} h^{-1}	4.54	2.21	1.41
	$q_{e,cal}$	Equilibrium capacity, mg g^{-1}	38.46	48.54	66.67
	R^2	Correlative coefficient	0.9992	0.9964	0.9972
Intraparticle diffusion	K_{p1} (10^{-1})	Rate constant, mg h$^{-1/2}$ g^{-1}	21.62	26.78	22.62
	C_1		6.53	8.48	13.26
	R_1^2	Correlative coefficient	0.9853	0.9554	0.981
	K_{p2} (10^{-1})	Rate constant, mg h$^{-1/2}$ g^{-1}	2.8	4.57	8.89
	C_2		26.57	27.08	31.65
	R_2^2	Correlative coefficient	0.832	0.9694	0.9651
	K_{p3} (10^{-1})	Rate constant, mg h$^{-1/2}$ g^{-1}	0.92	2.67	4.77
	C_3		33.47	35.03	42.68
	R_2^3	Correlative coefficient	0.8938	0.9021	0.9289
$q_{e,exp}$		Experimental data of the equilibrium capacity, mg g^{-1}	38.64	48.50	66.94

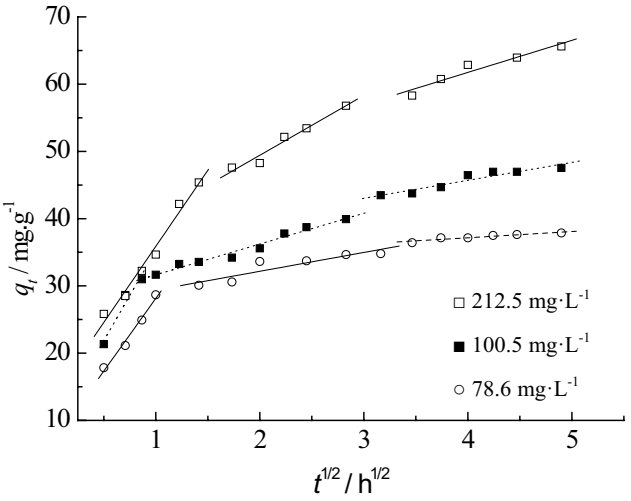

Fig. 7. Intraparticle diffusion model plots at different initial concentrations (T = 298 K, pH = 8.0 ± 0.1, rpm = 100).

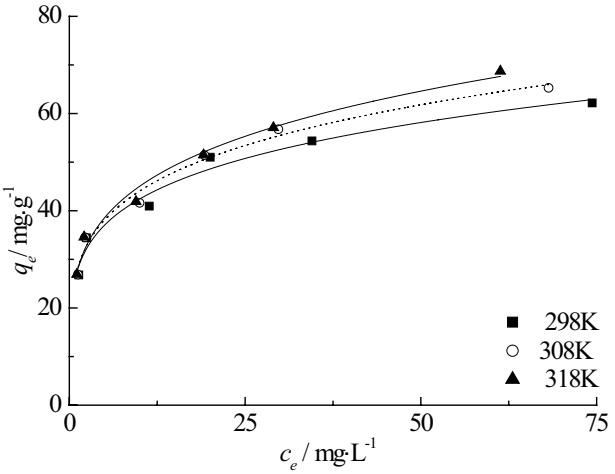

Fig. 8. Adsorption isotherms of CV on EMC (pH = 8.0 ± 0.1, contact time = 24 h, rpm = 100).

As expected, the rate constants K_p decreased from the external to intraparticle diffusion and to equilibrium due to the gradual occupation of pores and surface spaces by the CV molecules. And consequently, an increase in boundary thickness at the surface of EMC was observed. Similar discoveries were observed for other adsorption systems [44–46].

3.4. Adsorption isotherms

Equilibrium adsorption studies of CV were conducted at 298, 308 and 318 K and depicted in Fig. 8. The adsorption parameters obtained by non-linear regression analysis based on the Langmuir and Freundlich isotherms are listed in Table 1. According to Fig. 8 and Table 2, the adsorption capacity was found to increase slightly with increasing temperature from 298 to 318 K, which indicated that the adsorption of CV onto EMC maybe of endothermic nature. Furthermore, the increasing trend of adsorption with temperature is mainly due to the strength of adsorptive forces between the active sites of EMC and CV. The correlative coefficient R^2 values confirmed that the Langmuir isotherm exhibited a better fit to the equilibrium data (all > 0.985). It may be due to a homogenous distribution of active sites on the EMC surface since the Langmuir equation assumes that the surface is homogenous [22]. Based on electrostatic attractions, active sites are occupied by CV molecules and no more adsorption is possible on these sites. The Langmuir maximum adsorption capacity of EMC for CV listed in Table 1 was 71.43 mg g^{-1} at 318 K. n values of the Freundlich isotherm (all > 1) were high enough for CV adsorption onto EMC [47]. The heterogeneity of the adsorption is evaluated in terms of n value of the Freundlich model. The values of n were all greater than 1 and thereby indicated that non-linear heterogeneous adsorption also occurred in this process [23].

3.5. Thermodynamic studies

Different K_e values calculated using Eqs. (8)–(10) are listed in Table 3. The plots of $\ln(C_a/C_e)$ vs. C_a are given in Fig. 9.

Table 2
Langmuir and Freundlich isotherm constants of CV on EMC

T/K	Langmuir constants			Freundlich constants		
	q_{max}/mg g^{-1}	K_L/L mg^{-1}	R^2	n	k_f	R^2
298	64.10	0.2508	0.9938	5.17	27.28	0.9725
308	68.03	0.2402	0.9929	4.76	27.17	0.9796
318	71.43	0.2174	0.9857	4.13	25.19	0.9956

Table 3
K_e values of different methods

T(K)	K_L (L mg^{-1})	K_{e1} ($10^6 K_L$)	K_{e2} (K_p(R^2))	K_{e3} (2,000 K_L)	n
298	0.2464	246,400	475.13 (0.9574)	492.89	5.17
308	0.2402	240,200	402.70 (0.9624)	480.39	4.76
318	0.2174	217,400	350.44 (0.9441)	434.78	4.13

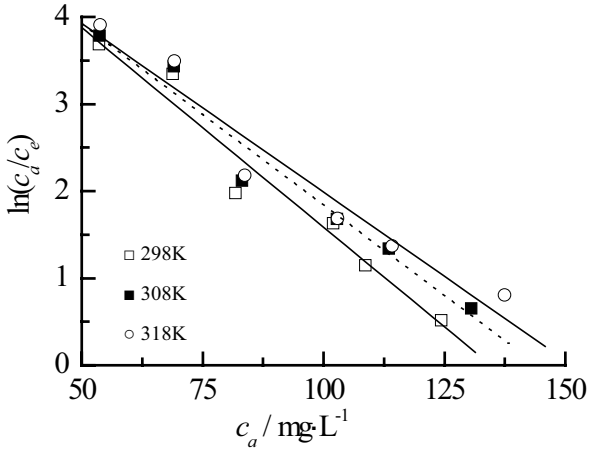

Fig. 9. Plot of $\ln(C_a/C_e)$ vs. C_a (pH = 8.0 ± 0.1, contact time = 24 h, rpm = 100).

Table 4
Thermodynamic properties of the systems tested

T (K)	K_L	ΔG (kJ mol^{-1})				$\Delta H(R^2)$ (kJ mol^{-1})		ΔS (J mol^{-1} K^{-1})	
		$K_{e1}(10^6K_L)$	K_{e2} (K_p)	K_{e3} (2,000 K_L)	n	K_{e2}	K_{e3}	K_{e2}	K_{e3}
298	3.47	–30.80	–15.27	–15.36	–12.81	–5.66 (0.9813)	–11.98 (0.988)	32.79	11.01
308	3.65	–31.73	–15.36	–15.81	–12.19				
318	4.03	–32.49	–15.49	–16.06	–10.92				

Table 5
Comparison of adsorption capacities of various adsorbents for CV

Absorbent	Langmuir q_{max} (mg g^{-1})	T (°C)	References
Moroccan pyrophyllite	13.88	50	[50]
Peanut hull	33.33	50	[51]
Raw corncob	33.50[b]	25	Present Work
Chitin nanowhiskers from shrimp shell	39.56	–	[52]
Terminalia arjuna sawdust	45.99[a]	–	[53]
CuO/meso-silica nanocomposite	52.9		[54]
EMC	71.43	45	Present Work
Gum arabic-cl-poly(acrylamide) nanohydrogel	90.9	–	[36]
Functionalized multi-walled carbon nanotube	100	–	[55]

[a]Equilibrium adsorption capacity at the optimum adsorbent dose and pH of 0.4 g L^{-1} and 7, respectively.
[b]Adsorption capacity of 33.50 mg g^{-1} was obtained under the following experimental conditions: 100 mL CV solution with the initial concentration of 95.62 mg L^{-1}, 0.2 g of raw corncob, 25°C of temperature and adsorption for 14 h. Under the same conditions, 42.51 mg g^{-1} of capacity was obtained by the EMC.

We considered the thermodynamic parameters calculated with K_{e2} trustful since the R^2 values were high enough (all near 0.95). The obtained K_{e3} calculated by the newly established method in Table 3 was pretty close to that of K_{e2}, we, therefore, believe the conversion of K_L by multiplying with 2,000 to get the dimensionless K_e is credible.

Thermodynamic parameters obtained using Eqs. (7)–(11) are presented in Table 4. As shown by Table 4, the applied equilibrium constants showed a significant impact on the values of ΔG. ΔG values calculated with K_{e1} were two-three times the values calculated with K_{e2}, K_{e3} (dimensionless) and n, and the latter were very close. The negative values of ΔG derived from the constants K_{e1}, K_{e2}, K_{e3} (dimensionless) and n revealed that the adsorption process was spontaneous [48], while the positive ΔG value calculated directly with K_L (L mg^{-1}) provided a completely opposite sign. Therefore, a diverse even contradictory result could be deduced about the spontaneity of the adsorption process. However, since EMC showed excellent adsorption capacity for CV, it can be concluded that the adsorption of CV onto EMC is spontaneous.

The negative ΔH values could hardly be assigned to an exothermic process because of the slightly increased adsorption capacity at a higher temperature. This phenomenon can be better explained by an increase of dye adsorption rate under higher temperature due to the existence of chemical reaction. The calculated positive values for ΔS reflected the affinity between CV and EMC and the increased randomness on the EMC surface. Similar results were reported in the biosorption process of Co(II) ions [49].

Different methods were chosen to calculate the thermodynamic parameters, but the choice of selecting the most appropriate one is still an open question. In this work, we developed a new method derived from K_L to calculate thermodynamic parameters, and the obtained ΔG was pretty close to that calculated by K_p.

3.6. Comparison of the q_{max} of various adsorbents

The Langmuir maximum CV adsorption capacities of different adsorbents are compared in Table 5. q_{max} of EMC for CV was 71.43 mg g^{-1}, which was comparable with other adsorbents. EMC could be used as a promising adsorbent for dye removal from aqueous solutions.

4. Conclusions

A novel EMC adsorbent from raw corncob was prepared and characterized, and the adsorption behaviors of CV onto EMC were investigated in batch mode. The adsorption capacity of the EMC was considerably impacted by pH, contact time, initial CV concentration and temperature. The equilibrium phenomenon can be well described by both Langmuir and Freundlich equations. The obtained q_{max} is 71.43 mg g^{-1} at 318 K estimated with the Langmuir isotherm model. A new method derived from the obtained Langmuir equilibrium constant K_L was first proposed to estimate the thermodynamics. The obtained negative values of ΔG demonstrated a spontaneous process of CV onto corncob. Kinetic equations

were used to analyze the adsorption kinetics at different initial CV concentrations and revealed that the kinetic data could be more properly elucidated by the pseudo-second-order kinetic model. The results of the study indicated that EMC can be used as a promising adsorbent for dye removal.

Acknowledgment

This work was supported by the Project Foundation of Chongqing Municipal Education Committee (KJ1600619).

References

[1] Y.H. Magdy, H. Altaher, Kinetic analysis of the adsorption of dyes from high strength wastewater on cement kiln dust, J. Environ. Chem. Eng., 6 (2018) 834–841.
[2] M. Saad, H. Tahir, J. Khan, U. Hameed, A. Saud, Synthesis of polyaniline nanoparticles and their application for the removal of Crystal Violet dye by ultrasonicated adsorption process based on response surface methodology, Ultrason. Sonochem., 34 (2017) 600–608.
[3] M. Goswami, P. Phuka, Enhanced adsorption of cationic dyes using sulfonic acid modified activated carbon, J. Environ. Chem. Eng., 5 (2017) 3508–3517.
[4] Y. Song, Y. Liu, S. Chen, H. Xu, Y. Liao, Sunset Yellow adsorption by peanut husk in batch mode, Fresenius Environ. Bull., 23 (2014) 1074–1079.
[5] Y. Song, Y. Liu, S. Chen, H. Qin, H. Xu, Carmine adsorption from aqueous solution by crosslinked peanut husk, Iran. J. Chem. Chem. Eng., 33 (2014) 69–77.
[6] F. Temesgen, N. Gabbiye, O. Sahu, Biosorption of reactive red dye (RRD) on activated surface of banana and orange peels: economical alternative for textile effluent, Surf. Interfaces, 12 (2018) 151–159.
[7] S. Banerjee, M.C. Chattopadhyaya, Adsorption characteristics for the removal of a toxic dye, tartrazine from aqueous solutions by a low cost agricultural by-product, Arabian J. Chem., 10 (2017) S1629–S1638.
[8] U.J. Etim, S.A. Umoren, U.M. Eduok, Coconut coir dust as a low cost adsorbent for the removal of cationic dye from aqueous solution, J. Saudi Chem. Soc., 20 (2016) S67–S76.
[9] S. Dardouri, J. Sghaier, A comparative study of adsorption and regeneration with different agricultural wastes as adsorbents for the removal of methylene blue from aqueous solution, Chin. J. Chem. Eng., 25 (2017) 1282–1287.
[10] Y. Miyaha, A. Lahrichi, M. Idrissi, A. Khilil, F. Zerrouq, Adsorption of methylene blue dye from aqueous solutions onto walnut shells powder: equilibrium and kinetic studies, Surf. Interfaces, 11 (2018) 74–81.
[11] S. Vafakhah, M.E. Bahrololoom, R. Bazarganlari, M. Saeedikhani, Removal of copper ions from electroplating effluent solutions with native corn cob and corn stalk and chemically modified corn stalk, J. Environ. Chem. Eng., 2 (2014) 356–361.
[12] O.E. Gamal, M.Y. Mohamed, A.A. Amany, Assessment of activated carbon prepared from corncob by chemical activation with phosphoric acid, Water Resour. Ind., 7–8 (2014) 66–75.
[13] G. Zhu, X. Deng, M. Hou, K. Sun, Y. Zhang, P. Li, F. Liang, Comparative study on characterization and adsorption properties of activated carbons by phosphoric acid activation from corncob and its acid and alkaline hydrolysis residues, Fuel Process. Technol., 144 (2016) 255–261.
[14] H. Ma, J. Li, W. Liu, M. Miao, B. Ceng, S. Zhu, Novel synthesis of a versatile magnetic adsorbent derived from corncob for dye removal, Bioresour. Technol., 190 (2015) 13–20.
[15] K.A. Riyadh, S.A. Ammar, Adsorption of organic pollutants from real refinery wastewater on prepared cross-linked starch by epichlorohydrin, Data Brief, 19 (2018) 1318–1326.
[16] C. Fan, Y. Zhang, Adsorption isotherms, kinetics and thermodynamics of nitrate and phosphate in binary systems on a novel adsorbent derived from corn stalks, J. Geochem. Explor., 188 (2018) 95–100.
[17] M.E. Brassesco, N.W. Valetti, G. Pico, Molecular mechanism of lysozyme adsorption onto chemically modified alginate guar gum matrix, Int. J. Biol. Macromol.,96 (2017) 111–117.
[18] J. Cao, J. Lin, F. Fang, M. Zhang, Z. Hu, A new absorbent by modifying walnut shell for the removal of anionic dye: kinetic and thermodynamic studies, Bioresour. Technol., 163 (2014) 199–205.
[19] S. Lagergren, About the theory of so-called adsorption of soluble substances, K. Sven. Vetensakad. Handl., 24 (1898) 1–39.
[20] Y.S. Ho, G. McKay, Pseudo-second order model for sorption processes, Process Biochem., 34 (1999) 451–465.
[21] W.J. Weber, J.C. Morris, Kinetics of adsorption on carbon from solution, J. Sanit. Eng. Div., 89 (1963) 31–60.
[22] I. Langmuir, The constitution and fundamental properties of solids and liquids, J. Am. Chem. Soc., 38 (1916) 2221–2295.
[23] H.M.F. Freundlich, Über die Adsorption in Lösungen, Z. Phys. Chem., 57U (1906) 385–470.
[24] N. Fallah, M. Taghizadeh, S. Hassanpour, Selective adsorption of Mo(VI) ions from aqueous solution using a surface-grafted Mo(VI) ion imprinted polymer, Polymer, 144 (2018) 80–91.
[25] A. Saraeian, A. Hadi, F. Raji, A. Ghassemi, M. Johnson, Cadmium removal from aqueous solution by low-cost native and surface modified *Sorghum x drummondii* (Sudangrass), J. Environ. Chem. Eng., 6 (2018) 3322–3331.
[26] K.A. Lin, Y. Hsie, Copper-based metal organic framework (MOF), HKUST-1, as an efficient adsorbent to remove *p*-nitrophenol from water, J. Taiwan Inst. Chem. Eng., 50 (2015) 223–228.
[27] E. Nishikawa, M.G.C. Silva, M.G.A. Vieira, Cadmium biosorption by alginate extraction waste and process overview in life cycle assessment context, J. Cleaner Prod., 178 (2018) 166–175.
[28] M.C. Stanciu, M. Nichifo, Influence of dextran hydrogel characteristics on adsorption capacity for anionic dyes, Carbohydr. Polym., 199 (2018) 75–83.
[29] N.T.T. Tu, T.V. Thien, P.D. Du, V.T.T. Chau, T.X. Mau, D.Q. Khieu, Adsorptive removal of Congo red from aqueous solution using zeolitic imidazolate framework–67, J. Environ. Chem. Eng., 6 (2018) 2269–2280.
[30] A. Kumar, H.M. Jena, Adsorption of Cr(VI) from aqueous phase by high surface area activated carbon prepared by chemical activation with $ZnCl_2$, Process Saf. Environ. Prot., 109 (2017) 63–71.
[31] D. Singh, S.K. Singh, N. Atar, V. Krishna, Amino acid functionalized magnetic nanoparticles for removal of Ni(II) from aqueous solution, J. Taiwan Inst. Chem. Eng., 67 (2016) 148–160.
[32] D.L. Postai, C.A. Demarchi, F. Zanatta, D.C.C. Melo, C.A. Rodrigues, Adsorption of rhodamine B and methylene blue dyes using waste of seeds of *Aleurites Moluccana*, a low cost adsorbent, Alexandria Eng. J., 55 (2016) 1713–1723.
[33] H.N. Tran, S. You, A. Hosseini-Bandegharaei, H. Chao, Mistakes and inconsistencies regarding adsorption of contaminants from aqueous solutions: a critical review, Water Res., 120 (2017) 88–116.
[34] Y. Song, H. Xu, J. Ren, Adsorption study for removal of sunset yellow by ethylenediamine-modified peanut husk, Desal. Wat. Treat., 57 (2016) 17585–17592.
[35] R. Gnanasambandam, A. Proctor, Determination of pectin degree of esterification by diffuse reflectance Fourier transform infrared spectroscopy, Food Chem., 15 (2000) 327–332.
[36] G. Sharma, A. Kumar, M. Naushad, A. Garcia-Perias, A.H. Al-Muhtaseb, A.A. Ghfar, V. Sharma, T. Ahamad, F.J. Stadler, Fabrication and characterization of Gum arabic-*cl*-poly(acrylamide) nanohydrogel for effective adsorption of crystal violet dye, Carbohydr. Polym., 202 (2018) 444–453.
[37] S. Shoukat, H.N. Bhatti, M. Iqbal, S. Noreen, Mango stone biocomposite preparation and application for crystal violet adsorption: a mechanistic study, Microporous Mesoporous Mater., 239 (2017) 180–189.

[38] Y. Bulut, H. Aydin, A kinetics and thermodynamics study of methylene blue adsorption on wheat shells, Desalination, 194 (2006)259–267.
[39] M.A. Abdel-Khalek, M.K.A. Rahman, A.A. Francis, Exploring the adsorption behavior of cationic and anionic dyes on industrial waste shells of egg, J. Environ. Chem. Eng., 5 (2017) 319–327.
[40] K.Y. Foo, Value-added utilization of maize cobs waste as an environmental friendly solution for the innovative treatment of carbofuran, Process Saf. Environ. Prot., 100 (2016) 295–304.
[41] F. Hemmati, R. Norouzbeigi, F. Sarbisheh, H. Shayesteh, Malachite green removal using modified sphagnum peat moss as a low-cost biosorbent: kinetic, equilibrium and thermodynamic studies, J. Taiwan Inst. Chem. Eng., 58 (2016) 482–489.
[42] M.H. Marzbali, M. Esmaieli, H. Abolghasemi, M.H. Marzbali, Tetracycline adsorption by H_3PO_4-activated carbon produced from apricot nut shells: a batch study, Process Saf. Environ. Prot., 102 (2016) 700–709.
[43] J. Ma, Y. Jia, Y. Jing, Y. Yao, J. Sun, Kinetics and thermodynamics of methylene blue adsorption by cobalt-hectorite composite, Dyes Pigm., 93 (2012) 1441–1446.
[44] M. Danish, T. Ahmad, S. Majeed, M. Ahmad, Z. Lou, P. Zhou, S.M.S. Iqubal, Use of banana trunk waste as activated carbon in scavenging methylene blue dye: kinetic, thermodynamic, and isotherm studies, Bioresour. Technol. Rep., 3 (2018) 127–137.
[45] S.J. Mousavi, M. Parvini, M. Ghorbani, Experimental design data for the zinc ions adsorption based on mesoporous modified chitosan using central composite design method, Carbohydr. Polym., 188 (2018) 197–212.
[46] Y. Song, S. Ding, S. Chen, H. Xu, M. Ye, J. Ren, Removal of malachite green in aqueous solution by adsorption on sawdust, Korean J. Chem. Eng., 32 (2015) 2443–2448.
[47] A.M. Aljeboree, A.N. Alshirifi, A.F. Alkaim, Kinetics and equilibrium study for the adsorption of textile dyes on coconut shell activated carbon, Arabian J. Chem., 10 (2017) S3381–S3393.
[48] R. Khamirchi, A. Hosseini-Bandegharaei, A. Alahabadi, S. Sivamani, A. Rahmani-Sani, T. Shahryari, I. Anastopoulos, M. Miri, H.N. Tran, Adsorption property of Br-PADAP-impregnated multiwall carbon nanotubes towards uranium and its performance in the selective separation and determination of uranium in different environmental samples, Ecotoxicol. Environ. Saf., 150 (2018) 136–143.
[49] S. Vilvanthan, S. Shanthakumar, Biosorption of Co(II) ions from aqueous solution using *Chrysanthemum indicum*: kinetics, equilibrium and thermodynamics, Process Saf. Environ. Prot., 96 (2015) 98–110.
[50] Y. Miyah, A. Lahrichi, M. Idrissi, S. Boujraf, H. Taouda, F. Zerrouq, Assessment of adsorption kinetics for removal potential of Crystal Violet dye from aqueous solutions using Moroccan pyrophyllite, J. Assoc, Arab Univ. Basic Appl. Sci., 23 (2017) 20–28.
[51] N. Tahir, H.N. Bhatti, M. Iqbal, S. Noreen, Biopolymers composites with peanut hull waste biomass and application for Crystal Violet adsorption, Int. J. Biol. Macromol., 94 (2017) 210–220.
[52] S. Gopi, A. Pius, S. Thoms, Enhanced adsorption of crystal violet by synthesized and characterized chitin nano whiskers from shrimp shell, J. Water Process Eng., 14 (2016) 1–8.
[53] S. Shakoor, A. Nasar, Adsorptive decontamination of synthetic wastewater containing crystal violet dye by employing *Terminalia arjuna* sawdust waste, Groundwater Sustainable Dev., 7 (2018) 30–38.
[54] Z. Liang, Z. Zhao, T. Sun, W. Shi, F. Cui, Enhanced adsorption of the cationic dyes in the spherical CuO/meso-silica nano composite and impact of solution chemistry, J. Colloid Interface Sci., 485 (2017) 192–200.
[55] V. Sabna, S.G. Thampi, S. Chandrakaran, Adsorption of crystal violet onto functionalized multi-walled carbon nanotubes: equilibrium and kinetics studies, Ecotoxicol. Environ. Saf., 134 (2016) 390–397.